Computational Geosciences (2019) 23:189–199
https://doi.org/10.1007/s10596-018-9792-y

ORIGINAL PAPER

A simple finite element method for elliptic bulk problems with embedded surfaces

Erik Burman[1] · **Peter Hansbo**[2] · **Mats G. Larson**[3]

Received: 6 September 2017 / Accepted: 12 October 2018 / Published online: 6 November 2018

Abstract

In this paper, we develop a simple finite element method for simulation of embedded layers of high permeability in a matrix of lower permeability using a basic model of Darcy flow in embedded cracks. The cracks are allowed to cut through the mesh in arbitrary fashion and we take the flow in the crack into account by superposition. The fact that we use continuous elements leads to suboptimal convergence due to the loss of regularity across the crack. We therefore refine the mesh in the vicinity of the crack in order to recover optimal order convergence in terms of the global mesh parameter. The proper degree of refinement is determined based on an a priori error estimate and can thus be performed before the actual finite element computation is started. Numerical examples showing this effect and confirming the theoretical results are provided. The approach is easy to implement and beneficial for rapid assessment of the effect of crack orientation and may for example be used in an optimization loop.

Keywords Darcy equation · Fracture · Embedded layer · Cut finite element methods

1 Introduction

New contributions In this contribution, we consider a basic elliptic problem with an embedded interface with high permeability, which may be used to model the pressure in a medium with cracks or the temperature in composite materials. Our approach is to use a continuous piecewise linear finite element space and simply insert this space into the weak formulation of the continuous problem which consists of a sum of a form on the bulk domain and a form on the interface. Note that the interface cuts through the mesh in an arbitrary way but we avoid using computations on cut elements and instead compensate the lack of regularity across the interface using a mesh which is adapted close to the interface. This approach leads to a scheme which is very easy to implement.

We derive a priori error estimates which shows that the meshsize for elements close to the interface $h_\Gamma \sim h^2$ where h is the global mesh parameter used in the bulk mesh. Such a pre-refinement of the mesh leads to optimal order a priori error estimates in terms of the global mesh parameter. Note that no adaptive algorithm is used instead we just split elements that intersect the interface until they are small enough. We start with a quasi uniform mesh and refine to obtain a conforming locally quasi uniform mesh for instance using an edge bisection algorithm.

In forthcoming work, we consider schemes using cut elements which does not require adaptive mesh refinement and also works for higher order elements. The method proposed here is however attractive due to its simplicity and may be an interesting alternative in situations where one does not need very accurate solutions for instance in the presence of uncertainties or very complicated networks of interfaces, or for optimization purposes.

Earlier work The model we use is essentially the one proposed by Capatina et al. [5]. More sophisticated models

✉ Peter Hansbo
Peter.Hansbo@ju.se

Erik Burman
e.burman@ucl.ac.uk

Mats G. Larson
mats.larson@umu.se

[1] Department of Mathematics, University College London, Gower Street, London WC1E 6BT, UK

[2] Department of Mechanical Engineering, Jönköping University, SE-55111 Jönköping, Sweden

[3] Department of Mathematics and Mathematical Statistics, Umeå University, SE-90187 Umeå, Sweden

have been proposed, e.g., in [1, 9, 10, 15], in particular allowing for jumps in the solution across the interfaces. To allow for such jumps, one can either align the mesh with the interfaces, as in, e.g., [11], or use extended finite element techniques, cf. [2, 5, 7, 8]. Our approach, using a continuous approximation, does not allow for jumps, but we shall return to this question in a companion paper.

The approach of superimposing lower dimensional structures independently of the mesh was recently introduced in the context of structural mechanics in [4, 6].

Outline In Section 2, we formulate the model problem, its weak form, and investigate the regularity properties of the solution; in Section 3, we formulate the finite element method; in Section 4, we derive error estimates; and in Section 5 we present numerical examples including a study of the convergence and a more applied example with a network of cracks.

2 Model Problem

Strong formulation Let Ω be a convex polygonal domain in $\mathbb{R}^d$, with $d = 2$ or 3. Let Γ be a smooth embedded interface in the interior of Ω without boundary. Then Γ partitions Ω into two subdomains Ω_1 and Ω_2, where Ω_2 is the domain enclosed by Γ. Let n_i be the exterior unit normal to Ω_i. See Fig. 1.

Consider the problem: find $u : \Omega \to \mathbb{R}$ such that

$$-\nabla \cdot a\nabla u = f, \quad \text{in } \Omega \tag{1}$$

$$[\![n \cdot a\nabla u]\!] - \nabla_\Gamma \cdot a_\Gamma \nabla_\Gamma u = f_\Gamma, \quad \text{on } \Gamma \tag{2}$$

$$[\![u]\!] = 0, \quad \text{on } \Gamma \tag{3}$$

$$u = 0, \quad \text{on } \partial\Omega \tag{4}$$

where $a|_{\Omega_i} = a_i$ are given constants, and $f \in L^2(\Omega)$, $f_\Gamma \in L^2(\Gamma)$ are given functions. We also used the notation $\nabla_\Gamma = P\nabla$ for the tangential gradient where $P = I - n \otimes n$ is the tangent projection. The jump in the primal variable across the interface is defined for $x \in \Gamma$ by $[\![v]\!] := \lim_{\epsilon \to 0^+}(v(x + \epsilon n_1) - v(x + \epsilon n_2))$ and that of the normal flux is defined by $[\![n \cdot a\nabla v]\!] = n_1 \cdot a_1 \nabla v_1 + n_2 \cdot a_2 \nabla v_2$, where we recall that $n_2 = -n_1$ on Γ.

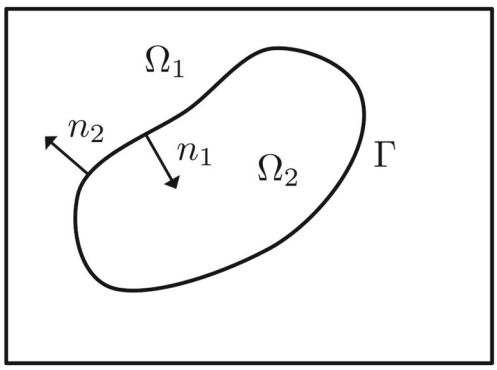

Fig. 1 The domains Ω_1, Ω_2, the interface Γ, and the unit exterior normals n_1 and n_2

Function spaces We adopt the usual notation $H^s(\omega)$ for the Sobolev space of order s on the set ω and we have the special spaces $H_0^1(\omega) = \{v \in H^1(\omega) : v = 0 \text{ on } \partial\omega\}$ and $L^2(\omega) = H^0(\omega)$. For a normed vector space V we let $\|\cdot\|_V$ denote the norm on V and we use the simplified notation $\|v\|_{L^2(\omega)} = \|v\|_\omega$. We denote the L^2-scalar product over $\omega \subset \mathbb{R}^d$ or $\omega \subset \mathbb{R}^{d-1}$ by $(\cdot, \cdot)_\omega$.

Weak formulation Multiplying (1) by $v \in V = H_0^1(\Omega) \cap H^1(\Gamma)$ and using Green's formula we obtain the weak form

$$\begin{aligned}
(f, v)_\Omega &= \sum_{i=1}^{2} \int_{\Omega_i} -\nabla \cdot a_i \nabla u_i \, , v_i \, d\boldsymbol{x} \\
&= \sum_{i=1}^{2} \int_{\Omega_i} a_i \nabla u_i \cdot \nabla v_i \, d\boldsymbol{x} - \int_\Gamma n_i \cdot a \nabla u_i \, v_i \, ds \\
&= \int_\Omega a\nabla u \cdot \nabla v \, d\boldsymbol{x} - \int_\Gamma [\![n \cdot a\nabla u]\!] \, v \, ds \\
&= \int_\Omega a\nabla u \cdot \nabla v \, d\boldsymbol{x} - \int_\Gamma (f_\Gamma + \nabla_\Gamma \cdot a_\Gamma \nabla_\Gamma u) \, v \, ds \\
&= \int_\Omega a\nabla u \cdot \nabla v \, d\boldsymbol{x} + \int_\Gamma a_\Gamma \nabla_\Gamma u \cdot \nabla_\Gamma v \, ds \\
&\quad - \int_\Gamma f_\Gamma \, v \, ds
\end{aligned} \tag{5}$$

where we used the fact that the boundary contributions on $\partial\Omega$ vanish due to the boundary condition and then we used (2). We thus arrive at the weak formulation: find $u \in V$ such that

$$A(u, v) = L(v) \qquad v \in V \tag{6}$$

where

$$A(u, v) = \int_\Omega a\nabla u \cdot \nabla v \, d\boldsymbol{x} + \int_\Gamma a_\Gamma \nabla_\Gamma u \cdot \nabla_\Gamma v \, ds \tag{7}$$

and

$$L(v) = \int_\Omega f \, v \, d\boldsymbol{x} + \int_\Gamma f_\Gamma \, v \, ds \tag{8}$$

Introducing the energy norm

$$|||v|||^2 = A(v, v) \tag{9}$$

on V, it follows using the Poincaré inequality $\|v\|_\Omega \lesssim \|\nabla v\|_\Omega$, which holds since $v = 0$ on $\partial\Omega$, and the trace inequality $\|v\|_\Gamma \lesssim \|v\|_{H^1(\Omega_2)}$, that

$$|||v|||^2 \sim \|v\|^2_{H^1(\Omega)} + \|v\|^2_{H^1(\Gamma)} \tag{10}$$

and hence $|||\cdot|||$ is a norm on V. The form A is a scalar product on V and by definition A is coercive and continuous on $|||\cdot|||$. Therefore it follows from the Lax-Milgram Lemma that there is a unique solution $u \in V$ to (6).

Regularity properties We have the elliptic regularity estimate

$$\|u\|_{H^2(\Omega_1\cup\Omega_2)} + \|u\|_{H^2(\Gamma)} \lesssim \|f\|_\Omega + \|f_\Gamma\|_\Gamma \tag{11}$$

where $\|u\|_{H^2(\Omega_1\cup\Omega_2)} := \|u\|_{H^2(\Omega_1)} + \|u\|_{H^2(\Omega_2)}$. To verify (11) we let $u_i \in H_0^1(\Omega_i)$ solve

$$\int_{\Omega_i} a_i \nabla u_i \cdot \nabla v \, d\boldsymbol{x} = \int_{\Omega_i} f\, v \, d\boldsymbol{x} \quad \forall v \in H_0^1(\Omega_i) \tag{12}$$

Then we have

$$\|u_i\|_{H^2(\Omega_i)} \lesssim \|f\|_{\Omega_i} \qquad i = 1, 2 \tag{13}$$

Observe that by the boundary conditions and the regularity of u_i we have that $\nabla_\Gamma u_i = 0$, $i = 1, 2$. Next writing $u = u_\Gamma + u_1 + u_2$ we find using the equation that $u_\Gamma \in V$ satisfies

$$\begin{aligned} -\nabla_\Gamma \cdot a_\Gamma \nabla_\Gamma u_\Gamma &= -\nabla_\Gamma \cdot a_\Gamma \nabla_\Gamma u \\ &= f_\Gamma + [\![n \cdot a \nabla u]\!] \\ &= f_\Gamma + n_1 \cdot (a_1 \nabla u_1 - a_2 \nabla u_2) \\ &\quad + [\![n \cdot a \nabla u_\Gamma]\!] \quad \text{on } \Gamma \end{aligned} \tag{14}$$

and

$$-\nabla \cdot a_i \nabla u_\Gamma = 0 \qquad \text{on } \Omega_i, i = 1, 2$$

Using (13) we conclude that

$$n_1 \cdot (a_1 \nabla u_1 - a_2 \nabla u_2)|_\Gamma \in H^{1/2}(\Gamma) \tag{15}$$

Furthermore, using that $u_\Gamma \in H^1(\Gamma)$, since $u_\Gamma \in V$, it follows that $u_\Gamma|_{\Omega_i} \in H^{3/2}(\Omega_i)$, $i = 1, 2$, and therefore

$$[\![n \cdot a \nabla u_\Gamma]\!] \in H^{1/2}(\Gamma) \tag{16}$$

Thus, using elliptic regularity we find that

$$u_\Gamma|_\Gamma \in H^2(\Gamma) \tag{17}$$

since the right hand side of (14) is in $L^2(\Gamma)$. Collecting the bounds we obtain the regularity estimate

$$\begin{aligned} &\|u_\Gamma\|_{H^2(\Gamma)} + \|u_\Gamma\|_{H^{5/2}(\Omega_1\cup\Omega_2)} + \|u_i\|_{H^2(\Omega_1\cup\Omega_2)} \\ &\quad \lesssim \|f\|_\Omega + \|f_\Gamma\|_\Gamma \end{aligned} \tag{18}$$

where we note that we have stronger control of u_Γ on the subdomains.

Remark Note that if we instead take $f \in H^{-1/2}(\Gamma)$ we will have $u_\Gamma|_\Gamma \in H^{3/2}(\Gamma)$ and $u_\Gamma \in H^2(\Omega_i)$ and the estimate

$$\|u\|_{H^2(\Omega_1\cup\Omega_2)} + \|u\|_{H^{3/2}(\Gamma)} \lesssim \|f\|_\Omega + \|f_\Gamma\|_{H^{-1/2}(\Gamma)} \tag{19}$$

3 The finite element method

To design a finite element method for the problem we use the classical approach restricting the weak formulation (6) to a suitably chosen finite dimensional subspace of V. To this end let

- $\mathcal{T}_h$ be a locally quasi uniform conforming mesh on Ω, consisting of shape regular simplices with element size h_T and let $h = \max_{T\in\mathcal{T}_h} h_T$ be the global mesh parameter.
- V_h be a finite element space consisting of continuous piecewise linear polynomials on $\mathcal{T}_h$.
- $\mathcal{T}_h(\Gamma)$ denote the set of elements intersected by the interface:

$$\mathcal{T}_h(\Gamma) := \{T \in \mathcal{T}_h : T \cap \Gamma \neq \emptyset\}$$

The finite element method takes the form: find $u_h \in V_h$ such that

$$A(u_h, v) = L(v) \qquad v \in V_h \tag{20}$$

4 Error estimates

4.1 Preliminaries

- Let ρ be the signed distance function associated with Γ, negative in Ω_1 and positive in Ω_2. We then have $n = \nabla\rho$ where $n = n_1$ is the unit normal direction exterior to Ω_1.
- For $\zeta > 0$ let define a tubular neighborhood around Γ by

$$U_\zeta(\Gamma) := \{x \in \Omega : \min_{x_\Gamma\in\Gamma} \|x - x_\Gamma\|_{\mathbb{R}^d} \leq \zeta\}. \tag{21}$$

- There is $\delta_0 > 0$ such that for each $x \in U_{\delta_0}(\Gamma)$ there is a unique point $p(x) \in \Gamma$ such that $\|x - p(x)\|_{\mathbb{R}^d}$ is minimal called the closest point. We also have the formula

$$p(x) = x - \rho(x) n(p(x)) \tag{22}$$

for the closest point mapping $p : U_{\delta_0}(\Gamma) \to \Gamma$.
- Let $v^e = v \circ p$ be the extension of v from Γ to $U_{\delta_0}(\Gamma)$. We then have

$$\|v^e\|_{U_\delta(\Gamma)} \lesssim \delta^{1/2} \|v\|_\Gamma \tag{23}$$

- The tangential gradient is defined by

$$\nabla_\Gamma v = P \nabla v^e \tag{24}$$

where we recall that $P(x) = I - n(x) \otimes n(x)$ is the projection onto the tangent plane $T_x(\Gamma)$ to Γ at x.

4.2 Interpolation

We introduce the following concepts.

- Let $\pi_h : L^2(\Omega) \to V_h$ be the Clément interpolant which satisfies the interpolation error estimate

$$\|u - \pi_h u\|_{H^s(T)} \lesssim h^{t-s} \|u\|_{H^t(\mathcal{N}_h(T))} \tag{25}$$

  $0 \le s \le t \le 2$, where $\mathcal{N}_h(T) \subset \mathcal{T}_h$ is the set of all elements which are node neighbors of T.
- In order to account for the fact that the exact solution u is not in regular across the interface we construct an interpolation operator which is modified close to the interface. Essentially, we interpolate on an extension of $u|_\Gamma$ in the neighborhood of Γ and on u outside of Γ. Let $\chi : [0, 1] \to [0, 1]$ be a smooth function such that $\chi = 0$ on $[2/3, 1]$, and $\chi = 1$ on $[0, 1/3]$. On $U_\delta(\Gamma)$ let $\chi_\delta(x) = \chi(|\rho(x)|/\delta)$ and on $\Omega \setminus U_\delta(\Gamma)$ let $\chi_\delta(x) = 0$. Define the interpolant

$$\begin{aligned} I_h v &= \pi_h(v(1 - \chi_\delta) + v^e \chi_\delta) \\ &= \pi_h(v + (v^e - v)\chi_\delta) \end{aligned} \tag{26}$$

  Note that with this construction we essentially interpolate u^e close to Γ and u outside of Γ.
- We consider meshes that are refined in the vicinity of the interface. More precisely, we assume that there are two mesh parameters h_Γ and h such that

$$\begin{cases} h_T \lesssim h_\Gamma & T \in \mathcal{N}_h(\mathcal{T}_h(\Gamma)) \\ h_T \lesssim h & T \in \mathcal{T}_h \setminus \mathcal{N}_h(\mathcal{T}_h(\Gamma)) \end{cases} \tag{27}$$

- We chose δ in the definition (26) of I_h in such a way that

$$\mathcal{N}_h(\mathcal{T}_h(\Gamma)) \subset U_{\delta/3}(\Gamma) \tag{28}$$

  which means that $\chi_\delta = 1$ on $\mathcal{N}_h(\mathcal{T}_h(\Gamma))$. We note that (28) then implies that we may take $\delta \sim h_\Gamma$ in the definition of χ_δ.

Remark We note that the total number of degrees of freedom N is related to the global mesh parameter as follows

$$N \sim h^{-d} + h_\Gamma^{-(d-1)} \sim h^{-d} + h^{-2(d-1)} \tag{29}$$

Thus, we find that for $d = 2$ we have $N \sim h^{-2}$, which is equivalent to the unrefined mesh, and for $d = 3$ we have $N \sim h^{-4}$, which is slightly more expensive compared to the unrefined mesh which scales as h^{-3}.

Lemma There is a constant such that

$$|||v - I_h v||| \lesssim h_\Gamma \|v\|_{H^2(\Gamma)} + (h + h_\Gamma^{1/2}) \|v\|_{H^2(\Omega_1 \cup \Omega_2)} \tag{30}$$

Proof Using the definition of I_h we have

$$v - I_h v = (v^e - v)\chi_\delta + (I - \pi_h)(v + (v^e - v)\chi_\delta) \tag{31}$$

and thus,

$$\begin{aligned} &\|\nabla(v - I_h v)\|_\Omega + \|\nabla_\Gamma(v - I_h v)\|_\Gamma \\ &\quad = \|\nabla((v^e - v)\chi_\delta)\|_\Omega \\ &\qquad + \|\nabla(I - \pi_h)(v + (v^e - v)\chi_\delta)\|_\Omega \\ &\qquad + \|\nabla_\Gamma(I - \pi_h)(v + (v^e - v)\chi_\delta)\|_\Gamma \\ &\quad = I + II + III \end{aligned} \tag{32}$$

Term *I*. Using the product rule and the triangle inequality

$$\begin{aligned} \|\nabla((v^e - v)\chi_\delta)\|_\Omega &\lesssim \|(\nabla(v^e - v))\chi_\delta\|_{U_\delta(\Gamma)} \\ &\quad + \|(v^e - v)(\nabla\chi_\delta)\|_{U_\delta(\Gamma)} \\ &\lesssim \|\nabla(v^e - v)\|_{U_\delta(\Gamma)} \\ &\quad + \delta^{-1}\|v^e - v\|_{U_\delta(\Gamma)} \\ &\lesssim \|(\nabla_\Gamma v)^e\|_{U_\delta(\Gamma)} + \|\nabla v\|_{U_\delta(\Gamma)} \\ &\quad + \|n^e \cdot \nabla v\|_{U_\delta(\Gamma)} \\ &\lesssim \delta^{1/2}\|\nabla_\Gamma v\|_\Gamma + \|\nabla v\|_{U_\delta(\Gamma)} \\ &\lesssim h_\Gamma^{1/2}\|v\|_{H^2(\Omega_1 \cup \Omega_2)} \end{aligned} \tag{33}$$

Here we used that by the properties of the extension there holds

$$\delta^{-1}\|v^e - v\|_{U_\delta(\Gamma)} \lesssim \|n^e \cdot \nabla v\|_{U_\delta(\Gamma)} \tag{34}$$

see the Appendix of [3] for a verification, and

$$\|w^e\|_{U_\delta(\Gamma)} \lesssim \delta^{\frac{1}{2}}\|w\|_\Gamma \tag{35}$$

which we applied with $w = \nabla_\Gamma v$. Furthermore, we used the bound

$$\|\nabla v\|_{U_\delta(\Gamma)} \lesssim \delta^{\frac{1}{2}} \sup_{t \in [-\delta, \delta]} \|\nabla v\|_{\Gamma_t} \tag{36}$$

where $\Gamma_t = \rho^{-1}(t) = \{x \in \mathbb{R}^d : \rho(x) = t\}$, for $|t| < \delta_0$, followed by the trace inequality

$$\begin{aligned} \|\nabla v\|_{\Gamma_t} &\le C_t \|v\|_{H^2(\Omega_i \setminus U_{|t|}(\Gamma))} \\ &\le \underbrace{\sup_{t \in [-\delta, \delta]} C_t}_{\le C} \|v\|_{H^2(\Omega_i)} \end{aligned} \tag{37}$$

where $i = 1$ for $t \in [-\delta, 0)$, $i = 2$ for $t \in [0, \delta]$, and finally $\delta \sim h_\Gamma$.

Term *II*. Using the interpolation error estimate (25) we obtain

$$\begin{aligned}
&\|\nabla(I-\pi_h)(v+(v^e-v)\chi_\delta)\|_\Omega \\
&\quad\lesssim \|\nabla(I-\pi_h)v\|_\Omega + \|\nabla(I-\pi_h)((v^e-v)\chi_\delta)\|_\Omega \\
&\quad\lesssim \|\nabla(I-\pi_h)v\|_\Omega + \underbrace{\|\nabla((v^e-v)\chi_\delta)\|_\Omega}_{I} \\
&\quad\lesssim (h_\Gamma^{1/2}+h)\|v\|_{H^2(\Omega_1\cup\Omega_2)} + h_\Gamma^{1/2}\|v\|_{H^2(\Omega_1\cup\Omega_2)}
\end{aligned} \tag{38}$$

Here, we used the estimate

$$\begin{aligned}
\|\nabla(I-\pi_h)v\|_\Omega &\lesssim \|\nabla(I-\pi_h)v\|_{\mathcal{N}_h(\mathcal{T}_h(\Gamma))} \\
&\quad + \|\nabla(I-\pi_h)v\|_{\mathcal{T}_h\setminus\mathcal{N}_h(\mathcal{T}_h(\Gamma))} \\
&\lesssim \|\nabla v\|_{\mathcal{N}_h(\mathcal{T}_h(\Gamma))} + h\|\nabla^2 v\|_{\mathcal{T}_h\setminus\mathcal{N}_h(\mathcal{T}_h(\Gamma))} \\
&\lesssim \delta^{1/2}\sup_{t\in[-\delta,\delta]}\|\nabla v\|_{\Gamma_t} \\
&\quad + h\|\nabla^2 v\|_{\mathcal{T}_h\setminus\mathcal{N}_h(\mathcal{T}_h(\Gamma))} \\
&\lesssim h_\Gamma^{1/2}\|v\|_{H^2(\Omega_1\cup\Omega_2)}
\end{aligned} \tag{39}$$

that is obtained using similar arguments as in (33).

Term *III*. Using the trace inequality

$$\|w\|^2_{\Gamma\cap T} \lesssim h^{-1}\|v\|^2_T + h\|\nabla v\|^2_T \tag{40}$$

see [12], the interpolation estimate (25), the fact (28), and finally the stability of the extension we find that

$$\begin{aligned}
&\|\nabla_\Gamma(I-\pi_h)(v+(v^e-v)\chi_\delta)\|^2_\Gamma \\
&\quad= \|\nabla_\Gamma((I-\pi_h)v^e)\|^2_\Gamma \\
&\quad\lesssim h_\Gamma^{-1}\|\nabla((I-\pi_h)(v+(v^e-v)\chi_\delta))\|^2_{\mathcal{T}_h(\Gamma)} \\
&\qquad + h_\Gamma\|\nabla^2((I-\pi_h)(v+(v^e-v)\chi_\delta))\|^2_{\mathcal{T}_h(\Gamma)} \\
&\quad\lesssim h_\Gamma\|\nabla^2(v+(v^e-v)\chi_\delta)\|^2_{\mathcal{N}_h(\mathcal{T}_h(\Gamma))} \\
&\quad\lesssim h_\Gamma\|v^e\|^2_{H^2(\mathcal{N}_h(\mathcal{T}_h(\Gamma)))} \\
&\quad\lesssim h_\Gamma^2\|v\|^2_{H^2(\Gamma)}
\end{aligned} \tag{41}$$

□

Remark Alternatively we may use a different extension operator and prove an interpolation estimate which requires less regularity as follows. We include some details for convenience

- There is a continuous extension operator

  $$H^s(\Gamma)\ni v\mapsto v^E\in H^{s+1/2}(\Omega) \tag{42}$$

  We construct v^E by first solving the Dirichlet problem $\Delta v^E = 0$ in Ω_2 and $v^E = v$ on Γ, for which we have the regularity estimate

  $$\|v^E\|_{H^{s+1/2}(\Omega_2)} \lesssim \|v\|_{H^s(\Gamma)}. \tag{43}$$

  Next, we extend v^E to $\mathbb{R}^d$ using a standard continuous extension operator $\mathcal{E}_{\Omega_2} : H^s(\Omega_2)\to H^s(\mathbb{R}^d)$, $s>0$, that is $v^E|_{\mathbb{R}^d\setminus\Omega_2} = \mathcal{E}_{\Omega_2}(v^E|_{\Omega_2})$.

- With v^E instead of v^e in the definition of I_h we derive the interpolation estimate

  $$|||v-I_hv||| \lesssim (h+h_\Gamma^{1/2})\|v\|_{H^2(\Omega)} + (h+h_\Gamma^{1/2})\|v\|_{H^2(\Gamma)} \tag{44}$$

  as follows. Term I and II can be estimated in the same way as above. For Term III we have the estimates

  $$\begin{aligned}
  &\|\nabla_\Gamma(I-\pi_h)(v+(v^E-v)\chi_\delta)\|^2_\Gamma \\
  &\quad= \|\nabla_\Gamma((I-\pi_h)v^E)\|^2_\Gamma \\
  &\quad\lesssim h_\Gamma^{-1}\|\nabla((I-\pi_h)(v+(v^E-v)\chi_\delta))\|^2_{\mathcal{T}_h(\Gamma)} \\
  &\qquad + h_\Gamma\|\nabla^2((I-\pi_h)(v+(v^E-v)\chi_\delta))\|^2_{\mathcal{T}_h(\Gamma)} \\
  &\quad\lesssim h_\Gamma\|\nabla^2(v+(v^E-v)\chi_\delta)\|^2_{\mathcal{N}_h(\mathcal{T}_h(\Gamma))} \\
  &\quad\lesssim h_\Gamma\|v^E\|^2_{H^2(\mathcal{N}_h(\mathcal{T}_h(\Gamma)))} \\
  &\quad\lesssim h_\Gamma\|v\|^2_{H^{3/2}(\Gamma)} \\
  &\quad\lesssim h_\Gamma\|v\|^2_{H^2(\Omega_2)}
  \end{aligned} \tag{45}$$

  where at last we used a trace inequality to pass from Γ to Ω_2.

4.3 Error estimates

Theorem The following error estimates hold

$$|||u-u_h||| \lesssim (h_\Gamma^{1/2}+h)\|u\|_{H^2(\Omega_1\cup\Omega_2)} + h_\Gamma\|u\|_{H^2(\Gamma)} \tag{46}$$

$$\begin{aligned}
\|u-u_h\|_\Omega + \|u-u_h\|_\Gamma &\lesssim h_\Gamma\|u\|_{H^2(\Omega_1\cup\Omega_2)} \\
&\quad + h^2\|u\|_{H^2(\Omega_1\cup\Omega_2)} + h_\Gamma^2\|u\|_{H^2(\Gamma)}
\end{aligned} \tag{47}$$

Proof **(46).** The proof follows immediately from Galerkin orthogonality and the interpolation error estimate

$$\begin{aligned}
|||u-u_h|||^2 &= A(u-u_h,u-u_h) \\
&= A(u-u_h,u-\pi_hu) \\
&\le |||u-u_h|||\,|||u-\pi_hu|||
\end{aligned} \tag{48}$$

and thus

$$\begin{aligned}
|||u-u_h||| &\le |||u-\pi_hu||| \lesssim (h_\Gamma^{1/2}+h)\|u\|_{H^2(\Omega_1\cup\Omega_2)} \\
&\quad + h_\Gamma\|u\|_{H^2(\Gamma)}
\end{aligned} \tag{49}$$

(47). For the L^2 estimate we obtain an error representation formula using the dual problem: find $\phi\in V$ such that

$$A(v,\phi) = (u-u_h,v)_\Omega + (u-u_h,v)_\Gamma \tag{50}$$

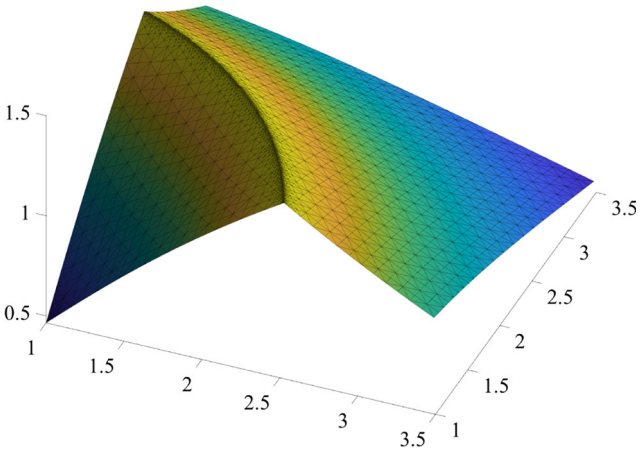

Fig. 2 Elevation of the solution on a locally refined mesh

for all $v \in V$, with $v = u - h_h$,

$$\begin{aligned}
&\|u-u_h\|_\Omega^2 + \|u-u_h\|_\Gamma^2 \\
&\quad = A(u-u_h,\phi) = A(u-u_h,\phi - I_h\phi) \\
&\quad \le |||u-u_h|||\,|||\phi - I_h\phi||| \\
&\quad \lesssim \left((h_\Gamma^{1/2}+h)\Big(\|u\|_{H^2(\Omega_1\cup\Omega_2)}\Big) + h_\Gamma\|u\|_{H^2(\Gamma)}\right) \\
&\qquad \times \left((h_\Gamma^{1/2}+h)\Big(\|\phi\|_{H^2(\Omega_1\cup\Omega_2)}\Big) + h_\Gamma\|\phi\|_{H^2(\Gamma)}\right) \\
&\quad \lesssim \left((h_\Gamma + h^2)\Big(\|u\|_{H^2(\Omega_1\cup\Omega_2)}\Big) + h_\Gamma^2\|u\|_{H^2(\Gamma)}\right) \\
&\qquad \times \left(\|u-u_h\|_\Omega^2 + \|u-u_h\|_\Gamma^2\right)^{1/2} \qquad (51)
\end{aligned}$$

where at last we used the elliptic regularity estimate (11). □

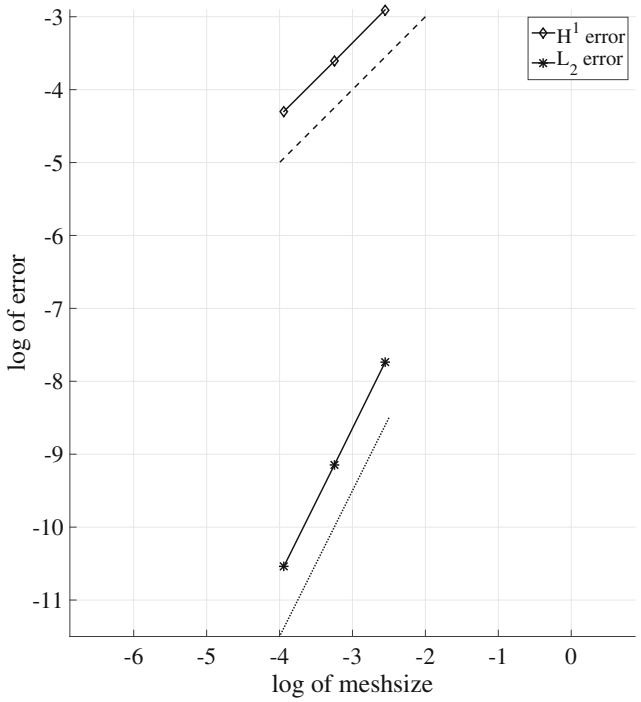

Fig. 3 Convergence on a locally refined mesh. Dashed line has inclination 1:1, and dotted line 2:1

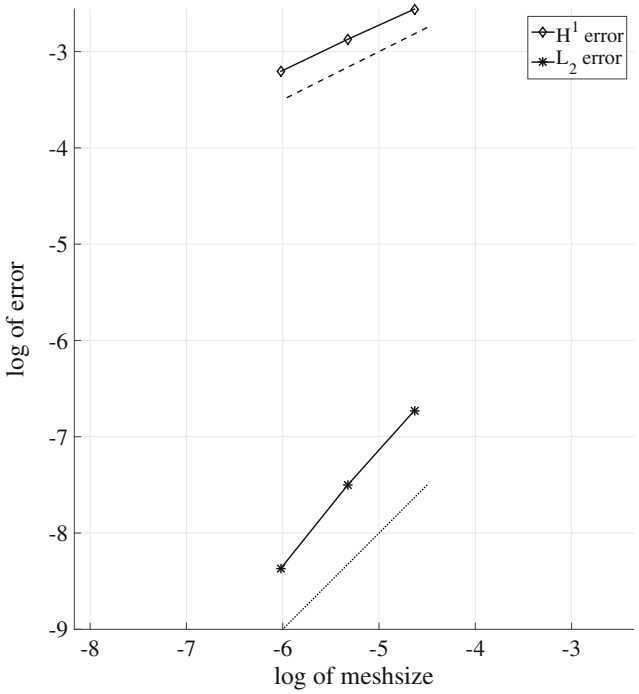

Fig. 4 Convergence on a globally refined mesh. Dashed line has inclination 1:2, and dotted line 1:1

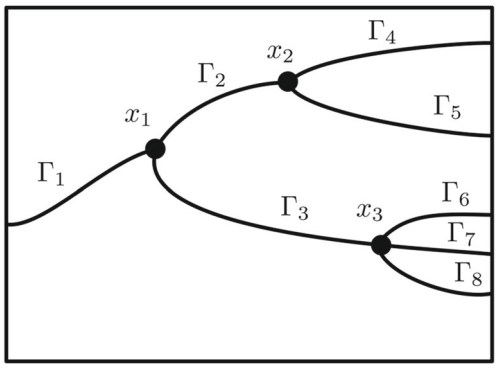

Fig. 5 Schematic figure of bifurcating cracks with nodes $\mathcal{N} = \{x_i\}_{i=1}^3$ and curves $\mathcal{G} = \{\Gamma_i\}_{i=1}^8$. The connectivity is described by the mappings I_N and I_G and we have for instance $I_N(3) = \{1, 3\}$ and $I_G(2) = \{2, 4, 5\}$

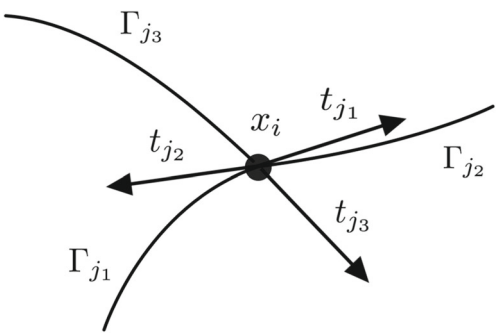

Fig. 6 Schematic figure of node x_i with its associated three curves Γ_k, and exterior unit tangents t_k at x_i for $k \in I_G(i) = \{j_1, j_2, j_3\}$

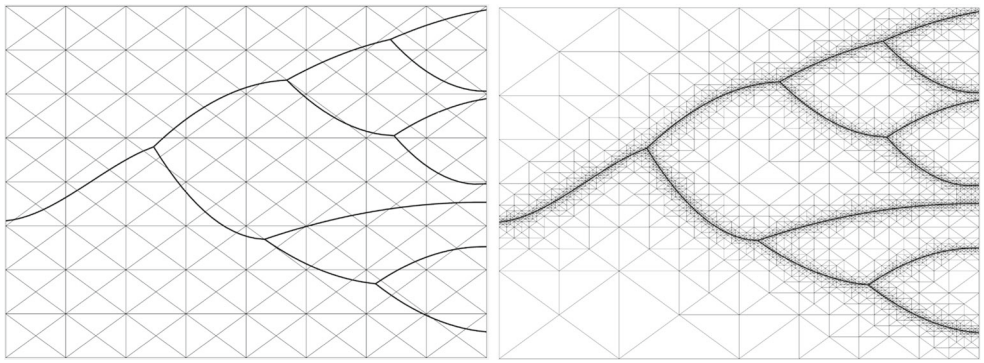

Fig. 7 Crack pattern modelled on a coarse and a locally refined mesh

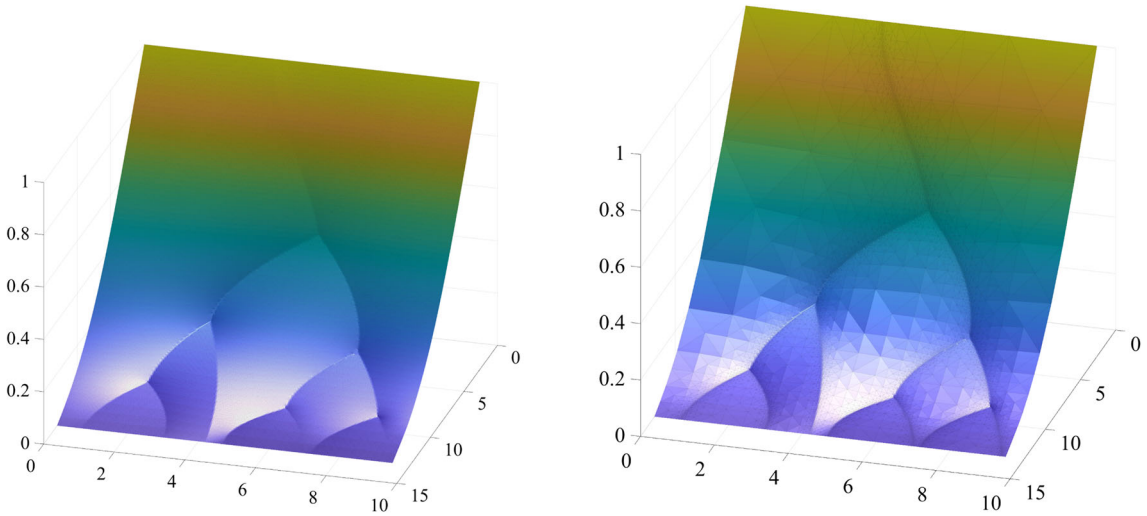

Fig. 8 Discrete solutions on a globally refined mesh and a mesh refined along the crack (smallest meshsize equal)

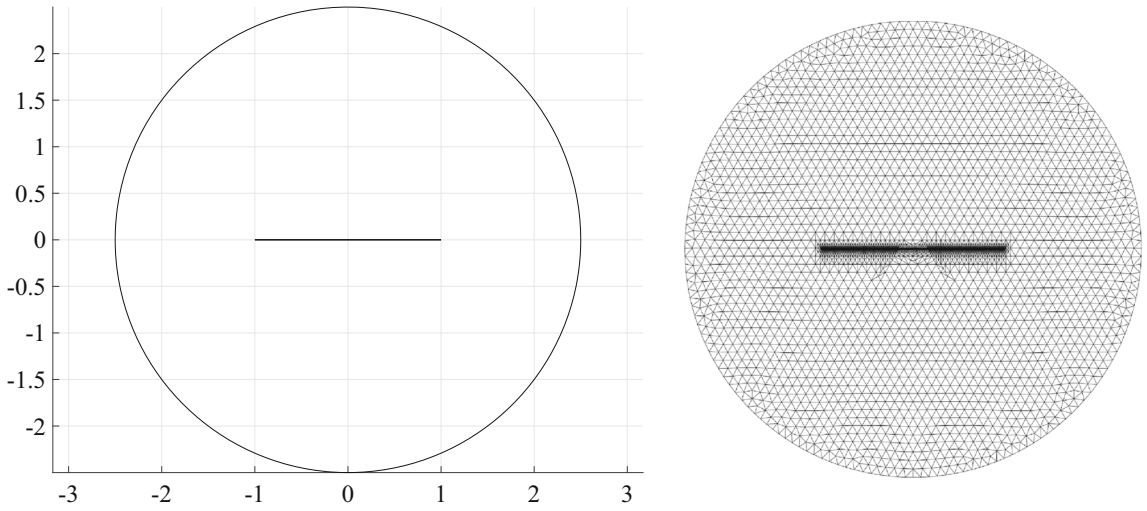

Fig. 9 Domain with crack and corresponding computational mesh (smallest meshsize 1/100 times largest meshsize)

5 Numerical examples

In this Section we give some basic examples of the performance of our method: we show that the convergence estimates are reflected in practice, we show that bifurcating cracks can be easily accommodated, and we solve a practical engineering problem of reservoir flow with a crack. More complex types of subsurface flows modelled with our approach can be found in the recent work [16].

5.1 A convergence study for a simple interface problem

We consider a problem with $f = 0$, $f_\Gamma = 1$, $a_1 = a_2 = a_\Gamma = 1$ on the domain

$$\Omega = (1, e^{5/4}) \times (1, e^{5/4})$$

with a crack at $\sqrt{(x^2 + y^2)} =: r = e$. The exact solution to this problem is given as

$$u_1 = \frac{\log(r)}{5}(4 + e), \quad 1 < r < e$$
$$u_2 = \frac{4 - 4e}{5}\left(\log(r) - \frac{5}{4}\right) + 1, \quad e < r < e^{5/4}$$

and this solution is applied as Dirichlet boundary conditions on $\partial\Omega$, corresponding to a solution depending only on r with $u = u_1 = 0$ at $r = 1$ and $u = u_2 = 1$ at $r = e^{5/4}$. We compare the convergence on a globally refined mesh with a mesh which is locally refined so that $h_\Gamma \leq h^2$ at Γ. The convergence is then checked in L^2 norm and H^1 (semi-) norm. In Fig. 2 we show the discrete solution on a given locally refined mesh. We note that optimal convergence is obtained at the cost of locally refining the mesh, Fig. 3, whereas a globally refined mesh gives suboptimal convergence in accordance with (46) and (47), Fig. 4.

5.2 A more complex example with a bifurcating crack

In this example, we illustrate the modeling capabilities of our approach with application to a more complex problem involving a bifurcating crack.

Model problem Let us for simplicity consider a two-dimensional problem with a one-dimensional crack Γ which can be described as a graph with nodes $\mathcal{N} = \{x_i\}_{i \in I_N}$ and edges $\mathcal{G} = \{\Gamma_j\}_{j \in I_G}$, where I_N, I_G are finite index sets, and each Γ_j is a curve between two nodes with indexes $I_N(j)$. For each $i \in I_N$, we let $I_G(i)$ be the set of indexes corresponding to curves for which x_i is an end point. See Figs. 5 and 6.

The governing equations are given by (1)–(4) together with two conditions at each of the nodes $x_i \in \mathcal{N}$, the continuity condition

$$u_{\Gamma_k}(x_i) = u_{\Gamma_l}(x_i) \qquad \forall k, l \in I_G(i) \tag{52}$$

and the Kirchhoff condition

$$\sum_{j \in I_G(i)} (t_{\Gamma_j} \cdot a_{\Gamma_j} \nabla_{\Gamma_j} u_{\Gamma_j})|_{x_j} = 0 \tag{53}$$

where $t_{\Gamma_j}(x_i)$ is the exterior tangent unit vector to Γ_j at x_i.

Finite element method Let $V_\Gamma = \{v \in C(\Gamma) : v \in H^1(\Gamma_j), j \in I_G\}$ and $V = H_0^1(\Omega) \cap V_\Gamma$. We proceed as in the derivation of the weak form in the standard case (5). However, when we use Green's formula on Γ, we proceed segment by segment as follows

$$\begin{aligned} &- \sum_{j \in I_G} \int_{\Gamma_j} \nabla_{\Gamma_j} \cdot a_{\Gamma_j} \nabla_{\Gamma_j} u\, v\, ds \\ &= \sum_{j \in I_G} \int_{\Gamma_j} a_{\Gamma_j} \nabla_{\Gamma_j} u \cdot \nabla_{\Gamma_j} v\, ds \\ &\quad - \sum_{j \in I_G} \sum_{i \in I_N(j)} (t_i \cdot a_{\Gamma_j} \nabla_{\Gamma_j} u\, v)\big|_{x_i} \\ &= \sum_{j \in I_G} \int_{\Gamma_j} a_{\Gamma_j} \nabla_{\Gamma_j} u \cdot \nabla_{\Gamma_j} v\, ds \end{aligned} \tag{54}$$

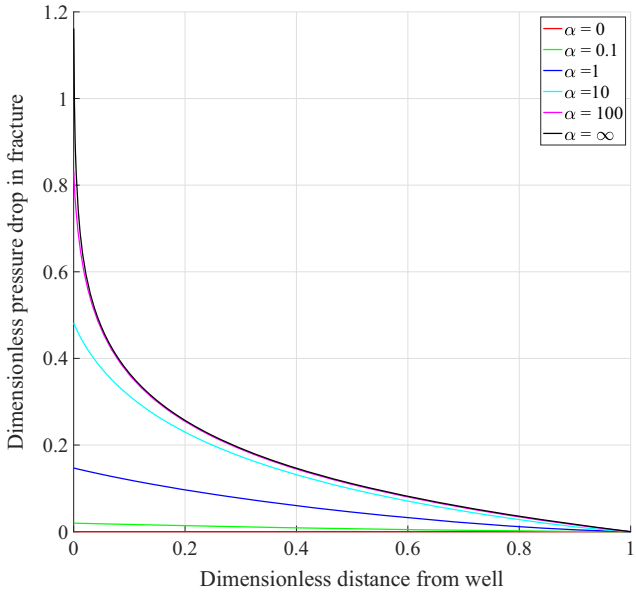

Fig. 10 Pressure drop as a function of distance from the well for varying α

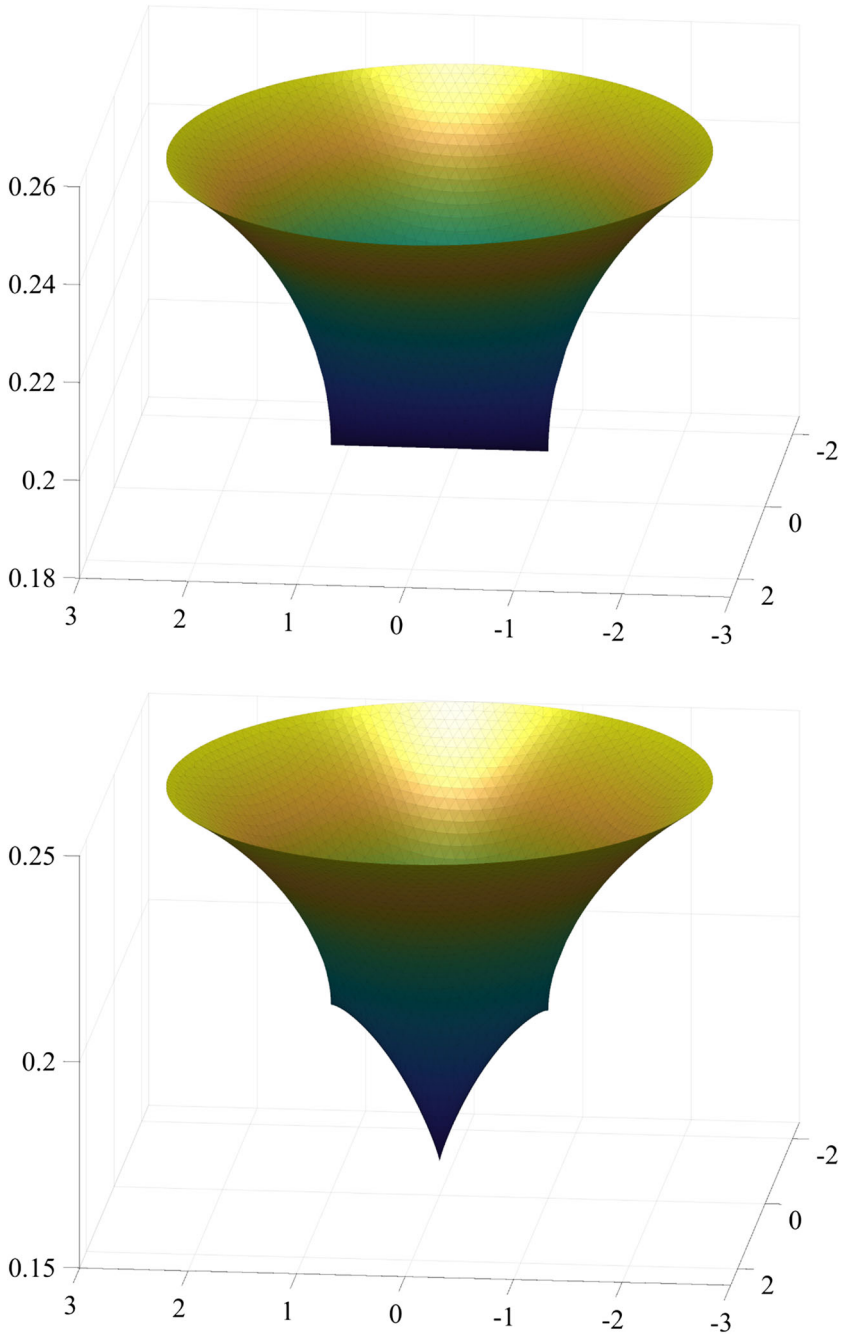

Fig. 11 Elevation of the pressure distrubution for α equal zero (top) and for α equal one (bottom)

where we changed the order of summation and used the Kirchhoff condition (53) together with the fact v is continuous to conclude that

$$\sum_{j\in I_G}\sum_{i\in I_N(j)}(t_i\cdot a_{\Gamma_j}\nabla_{\Gamma_j}u\,v)\big|_{x_i}=$$
$$\sum_{i\in I_N(j)}\sum_{j\in I_G}(t_i\cdot a_{\Gamma_j}\nabla_{\Gamma_j}u\,v)\big|_{x_i}=$$
$$\sum_{i\in I_N(j)}\underbrace{\Big(\sum_{j\in I_G}(t_i\cdot a_{\Gamma_j}\nabla_{\Gamma_j}u)|_{x_i}\Big)}_{=0}v(x_i)=0 \tag{55}$$

Thus, we conclude that:

- The weak formulation is precisely the same in the bifurcating crack case as in the standard case (6).
- Since $V_h\subset V$, the method also takes the same form as in the standard case (20) in this more complex situation.

The similar derivation can be performed for a two-dimensional bifurcating crack embedded into $\mathbb{R}^3$ (see [13] for further details).

Numerical example The crack pattern is modeled using a polygonal chain interpolating higher order curves with each

part of the chain of length $h/10$. The intersection points with element sides are computed and a new polygonal chain containing the old one cut by the intersection points is constructed. In Fig. 7, we show the effect on a coarse mesh and on a locally refined mesh. We now compute two different solutions using global refinement and local refinement. We use local refinement at Γ until the smallest meshsize equals that of the globally refined model. In Fig. 8, we give the computed solutions using these two approaches. Here $a_1 = a_2 = 1$ and $a_\Gamma = 100$, $f = f_\Gamma = 0$, and we impose, on the domain $\Omega = (0, 13) \times (0, 9.5)$, $u = 1$ at $x = 0$ and $u = 0$ at $x = 13$ and homogeneous Neumann boundary conditions at $y = 0$ and $y = 9.5$. The corresponding solution with $\alpha_\Gamma = 0$ is thus a plane.

5.3 A practical example of reservoir flow

In order to show the modeling capabilities of our approach on a classical problem, we consider the case of a well with a horizontal crack into a cylindrical reservoir from [17]. The cylindrical reservoir has a central well which on both sides in intersected by a crack, see Fig. 9. The permeability in the crack is allowed to vary according to

$$\alpha := \frac{\pi a L}{a_\Gamma}$$

where L is the total length of the crack and α is to be chosen; cf. [17] where α is described as "the ratio of the ability of the formation to carry fluid into the well to the ability of the fracture to carry fluids into the well" (note that the thickness of the crack is hidden in a_Γ in our formulation). The flow model is Darcy's law of creeping flow, and thus u plays the role of pressure.

For simplicity, we model the well by a point source term which is calibrated against values for $\alpha = 1$ in [17], and the pressure is assumed constant ($u = 0.25$) at the outer boundary of the reservoir. As can be seen in Fig. 9, the radius of the reservoir is $r = 2.5$ and the total length of the crack is $L = 2$; we fix $a = 1$. We then plot in Fig. 10, the computed relative pressure drop from the crack tip to the well as a function of distance from the well. The results agree with those of [17] in spite of the very basic model. In Fig. 11, we show the pressure distribution for the choices $\alpha = 0$ and $\alpha = 1$, where we note the changing pressure distribution in the crack.

This problem was also solved with explicit modelling of the crack using an XFEM–approach in [14] with similar results.

6 Concluding remarks

We suggest a continuous finite element method with superimposed lower dimensional features modeling interfaces. The effect of these are computed using the higher dimensional basis functions and added to the stiffness matrix so as to yield further "stiffness" to the problem. Due to the fact that we cannot resolve kinks in the normal derivative across the interface, we do not obtain optimal convergence orders. We propose a simple adaptive scheme based on an a priori error estimate which guides the choice of optimal local mesh size, to improve the local accuracy, regaining the optimal order of convergence. The resulting scheme is very simple and computationally expedient for many applications such as when optimization of the position of interfaces is of interest, or for coupling different flow models, cf. the recent work [16] where convection problems in the cracks are considered.

Funding information This research was supported in part by the Swedish Foundation for Strategic Research Grant No. AM13-0029, the Swedish Research Council Grants Nos. 2011-4992, 2013-4708, and the Swedish Research Programme Essence. The first author was supported in part by the EPSRC grant EP/P01576X/1.

References

1. Angot, P., Boyer, F., Hubert, F.: Asymptotic and numerical modelling of flows in fractured porous media. ESAIM: Math. Model. Numer. Anal. **43**(2), 239–275 (2009)
2. Burman, E., Claus, S., Hansbo, P., Larson, M.G., Massing, A.: CutFEM: discretizing geometry and partial differential equations. Internat. J. Numer. Methods Engrg. **104**(7), 472–501 (2015)
3. Burman, E., Hansbo, P., Larson, M.G.: A cut finite element method with boundary value correction. Math. Comp. **87**(310), 633–657 (2018)
4. Burman, E., Hansbo, P., Larson, M.G.: A simple approach for finite element simulation of reinforced plates. Finite Elem. Anal Des. **142**, 51–60 (2018)
5. Capatina, D., Luce, R., El-Otmany, H., Barrau, N.: Nitsche's extended finite element method for a fracture model in porous media. Appl Anal. **95**(10), 2224–2242 (2016)
6. Cenanovic, M., Hansbo, P., Larson, M.G.: Cut finite element modeling of linear membranes. Comput. Methods Appl. Mech Engrg. **310**, 98–111 (2016)
7. D'Angelo, C., Scotti, A.: A mixed finite element method for Darcy flow in fractured porous media with non-matching grids. ESAIM: Math. Model. Numer. Anal. **46**(2), 465–489 (2012)
8. Del Pra, M., Fumagalli, A., Scotti, A.: Well posedness of fully coupled fracture/bulk Darcy flow with XFEM. SIAM J. Numer Anal. **55**(2), 785–811 (2017)
9. Formaggia, L., Fumagalli, A., Scotti, A., Ruffo, P.: A reduced model for Darcy's problem in networks of fractures. ESAIM: Math. Model. Numer. Anal. **48**(4), 1089–1116 (2014)

10. Frih, N., Roberts, J.E., Saada, A.: Modeling fractures as interfaces: a model for Forchheimer fractures. Comput. Geosci. **12**(1), 91–104 (2008)
11. Hægland, H., Assteerawatt, A., Dahle, H.K., Eigestad, G.T., Helmig, R.: Comparison of cell- and vertex-centered discretization methods for flow in a two-dimensional discrete-fracture-matrix system. Adv. Water Resour. **32**(12), 1740–1755 (2009)
12. Hansbo, A., Hansbo, P., Larson, M.G.: A finite element method on composite grids based on Nitsche's method. ESAIM: Math. Model. Numer. Anal. **37**(3), 495–514 (2003)
13. Hansbo, P., Jonsson, T., Larson, M.G., Larsson, K.: A Nitsche method for elliptic problems on composite surfaces. Comput. Methods Appl. Mech. Engrg. **326**, 505–525 (2017)
14. Huang, H., Long, T.A., Wan, J., Brown, W.P.: On the use of enriched finite element method to model subsurface features in porous media flow problems. Comput. Geosci. **15**, 721–736 (2011)
15. Martin, V., Jaffré, J., Roberts, J.E.: Modeling fractures and barriers as interfaces for flow in porous media. SIAM J. Sci. Comput. **26**(5), 1667–1691 (2005)
16. Odsæter, L.H., Kvamsdal, T., Larson, M.G.: A simple embedded discrete fracture-matrix model for a coupled flow and transport problem in porous media. Comput. Methods Appl. Mech. Engrg. (to appear), arXiv:1803.03423 (2018)
17. Prats, M.: Effect of vertical fractures on reservoir behavior—incompressible fluid case. SPE J. **1**(2), 105–118 (1961)